Site-specific Photo-oxidation of the Isolated Adenosine-5′-triphosphate Dianion Determined by Photoelectron Imaging

Maria Elena Castellani[†1], Davide Avagliano[†2], Leticia González[*2], and Jan R. R. Verlet[*1]

[1]*Department of Chemistry, Durham University, DH1 3LE Durham, United Kingdom.*

[2]*Institute of Theoretical Chemistry, Faculty of Chemistry, University of Vienna, Währinger Str. 17 1090 Vienna, Austria.*

[†]equal contributions.

Correspondence:

[*] leticia.gonzalez@univie.ac.at

[*] j.r.r.verlet@durham.ac.uk

Abstract

Photoelectron imaging of the isolated adenosine-5′-triphosphate dianion excited to the $^{1}\pi\pi^{*}$ states reveals that electron emission is predominantly parallel to the polarization axis of the light and arises from sub-picosecond electron tunneling through the repulsive Coulomb barrier (RCB). The computed RCB shows that the most probable electron emission site is on the amino group of adenine. This is consistent with the photoelectron imaging: excitation to the $^{1}\pi\pi^{*}$ states leads to an aligned ensemble distributed predominantly parallel to the long axis of adenine, the subsequent electron tunneling site is along this axis, and the negatively charged phosphate groups guide the outgoing electron mostly along this axis at long range. Imaging electron tunneling from polyanions combined with computational chemistry may offer a general route to probing the intrinsic photo-oxidation site and dynamics as well as overall structure of complex isolated species.

TOC graphic

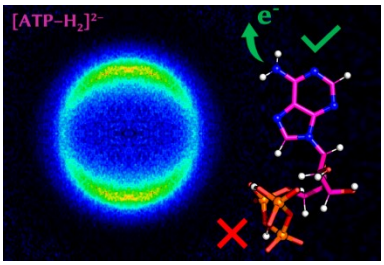

Keywords velocity map imaging; repulsive Coulomb barrier; ultrafast dynamics; tunneling

Photo-oxidation is an important source of biological damage, especially in DNA and its derivatives. All the nucleobases possess bright $^1\pi\pi^*$ states that can readily absorb ultraviolet light. Adenine in particular is a common nucleobase as it is present not only as one of the four DNA bases, but also in adenosine triphosphate (ATP) and nicotinamide adenine dinucleotide, which are central to cell energy distribution and to metabolism, respectively.[1, 2] To gain an understanding of the intrinsic photo-response of such molecules, gas-phase spectroscopy, in conjunction with electronic structure theory, has played an important role.[3, 4] For example, gas-phase environments have been used to probe: the decay dynamics of photo-excited nucleobases,[5-8] nucleotides[9] and oligonucleotides;[10] the ionization potential of the nucleobase in nucleotides;[9, 11] their geometric structures;[12-16] and their photo-dissociation products.[17, 18] The phosphate groups render most nucleotide derivatives negatively charged, and therefore multiple phosphates lead to polyanions. While ubiquitous in the condensed phase, a polyanion of charge Q can also exist in the gas-phase, but with the unique property that oxidation leads to a repulsive Coulomb barrier (RCB) between the departing electron and the remaining molecule with overall charge $Q - 1$.[19-22] Here, we exploit the unique properties of the RCB to determine the location of photo-oxidation in isolated doubly-deprotonated adenosine-5′-triphosphate dianions, $[ATP–H_2]^{2–}$, and as a crude probe of its molecular structure.

The electronic RCB arises from a balance between short-range attraction and long-range repulsion and has been extensively studied both theoretically[20, 21, 23] and experimentally.[22, 24] The latter has been conveniently enabled by photoelectron (PE) spectroscopy of the polyanion.[19, 22, 25-27] Consider a dianion, as in the case of $[ATP–H_2]^{2–}$. In the absence of photo-excited states, the RCB height shown in Figure 1(a) can be directly measured from an electron kinetic energy (eKE) cut-off in the PE spectra below which a PE cannot be emitted. If an excited state of the dianion lies below the RCB but higher than the adiabatic detachment energy of the dianion (ADE), then the excited state will be a resonance and will be metastable with respect to electron tunneling through the RCB. This scenario is shown in

Figure 1(a). The tunneling lifetime can be directly measured using time-resolved PE spectroscopy.[28] Moreover, the RCB is not isotropic and depends on the relative location of the charged sites with respect to the departing electron. This anisotropy can be clearly seen in the computation of the RCB and it can, in principle, be probed experimentally through PE imaging.[29] However, to do so requires a connection between the laboratory and molecular frames of reference, as the experiment probes only the laboratory-frame PE angular distribution. Such a connection can be most conveniently attained through photo-excitation of a chromophore with a known transition dipole moment, as has been shown for a model dianion.[30] Whilst the PE spectroscopy of polyanions has been predominantly an academic curiosity, there have been some PE spectroscopic measurements of polyanionic DNA fragments.[17, 31-39] In particular, Schinle *et al*.[34] performed a study of adenosine diphosphate, $[ADP–H_2]^{2–}$, and $[ATP–H_2]^{2–}$. For the latter, they observed no PE emission for excitation at 4.66 eV, although the photo-detachment action spectrum by Cercola *et al*.[17] clearly suggests there should be. Here, we observe this emission, show that it arises from resonance tunneling, and, with the aid of electronic structure calculations, reveal that photo-oxidation leads to electron emission from the amino group of adenine.

Figure 1(b) shows the PE spectrum of mass-selected $[ATP–H_2]^{2–}$, taken with 4.66 eV light pulses derived from either a nanosecond laser (~5 ns pulse duration) or a femtosecond laser (~80 fs pulse duration). The PE spectra using the different light sources are essentially indistinguishable and show a dominant detachment feature that peaks at eKE = 0.55 eV, with a slight shoulder at higher eKE. The PE spectra were obtained from their respective PE images, an example of which is shown inset in Figure 1(b). The PE feature at eKE = 0.55 eV is correlated with the intense and anisotropic inner ring. The anisotropy of this feature peaks parallel to the polarization axis of the light, $\boldsymbol{\varepsilon}$. The PE angular distribution, $I(\theta)\ \alpha\ 1 + \frac{1}{2}\beta_2(3\cos^2(\theta) - 1)$, where θ is the angle between $\boldsymbol{\varepsilon}$ and the velocity vector of the emitted electron, can be quantified using the anisotropy parameter, β_2.[40-42] For the dominant feature at eKE = 0.55 eV, β_2 = +0.69±0.07.

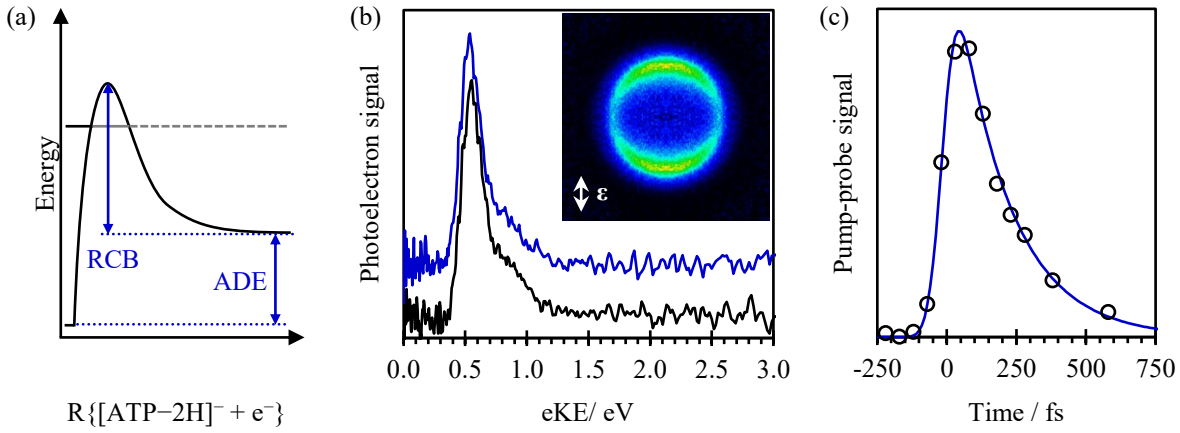

Figure 1: (a) Schematic of repulsive Coulomb barrier indicating its height (RCB) as a function of the distance between $[ATP–H_2]^-$ and the free electron, and the adiabatic detachment energy (ADE). (b) Photoelectron spectra of $[ATP–H_2]^{2-}$ taken at 4.66 eV with femtosecond (blue) and nanosecond (black) light pulses. Inset is a photoelectron image of $[ATP–H_2]^{2-}$ taken at 4.66 eV with nanosecond light pulses, with the polarization vector, **ε**, indicated. (c) Integrated pump-probe photoelectron signal following excitation to $^1\pi\pi^*$ states.

Schinle *et al.*[34] determined the adiabatic and vertical detachment energy of $[ATP–H_2]^{2-}$ to be 3.35±0.11 eV and 4.01±0.08 eV, respectively, and estimated the RCB to have a height of ~1.9 eV. Accordingly, the PE spectrum in Figure 1(b) would arise from resonance tunneling. We have verified this using time-resolved PE spectroscopy, which probed the initially excited state pumped at 4.66 eV with a 1.55 eV probe photon. The probe detaches a fraction of the excited state population generating electron signal at higher eKE. Concomitantly, the peak at 0.55 eV depletes as less population is available to tunnel. The integrated time-resolved PE signal over the energy range $0.9 < eKE < 2.0$, which probes the excited state population as a function of pump-probe delay, t, is shown in Figure 1(c), together with a fit to the data. The measured excited state lifetime is 190±30 fs. This decay depends on the electron tunneling lifetime, τ_{tun}, as well as any other decay processes that may compete, such as internal conversion that is known to be fast in adenine following excitation to the $^1\pi\pi^*$ states.[5, 6] Unfortunately,

the signal-to-noise in the time-resolved PE spectra was insufficient to analyze the data further. However, Cercola *et al.*[17] have measured the relative quantum yields of electron emission and photo-dissociation. Assuming a simple competitive 1st order kinetic model might then suggest that τ_{tun} is ~2.5 times the observed lifetime, such that we can estimate that τ_{tun} ~ 475 fs.

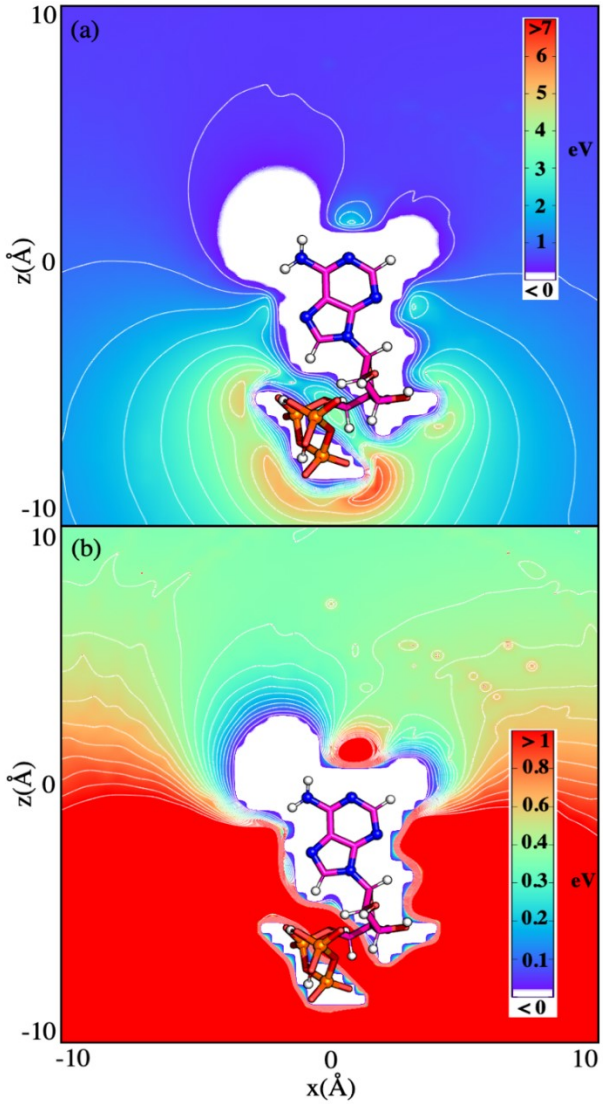

Figure 2: (a) Repulsive Coulomb barrier (RCB) for $[ATP–H_2]^-$ + e^- in the plane passing through the calculated transition dipole moment of the excitation to the $^1\pi\pi^*$ state and including the adenine ring; each contour line represents an increment of 1 eV. (b) Map scaled to a maximum RCB of 1 eV; each contour line represents an increment of 0.05 eV. RCB maps are computed at MP2/def2-SVP level of theory.

Figure 2 shows the computed RCB for $[ATP–H_2]^- + e^-$ in the *xz* plane containing the adenine ring system, as shown. Details of the calculation of the RCB are given in supporting information (section S1.2), as well as a larger region of the plane (Figure S2). The loss of a π electron from adenine results in an RCB that is highest near the phosphate groups where most of the negative charge resides. However, also on adenine itself, the potential energy is highly structured. The lowest energy saddle-point of the RCB can be found at the amino group, as more clearly shown in Figure 2(b), and has a computed barrier height of 0.57 eV. Although this is different from the estimated 1.9 eV RCB by Schinle *et al*.[34], caution should be applied regarding the previous PE spectrum. Firstly, the PE spectrum by Schinle *et al*. was taken at a photon energy of 6.42 eV, which is likely to be resonant with excited states not just on the nucleobase, but also the sugar and phosphate. It has been shown that the presence of resonances can lead to significant complications in terms of assigning the RCB from the PE spectrum.[22] Secondly, at a photon energy of 6.42 eV, electron emission (direct or by tunneling) can arise from several sites of $[ATP–H_2]^{2–}$ and it is not known *a priori* which one results in the strongest signal.[11] In the present experiment, the photon energy of 4.66 eV is only resonant with excited states localized on the nucleobase such that the electron is removed exclusively from the nucleobase.[43] In a separate experiment, we focused the femtosecond 4.66 eV light in the interaction region to obtain the 2-photon resonance-enhanced PE spectrum shown in Figure 3(a). This shows an onset of the eKE signal at ~5.2 eV, which yields the ADE associated with the nucleobase: $ADE_A = 2 \times 4.66 – 5.2 = 4.1$ eV. However, the highest occupied molecular orbital is also on the nucleobase, so this ADE_A measured is probably equivalent to the ADE of $[ATP–H_2]^{2–}$. The computed RCB is consistent with our measurements. Given $\tau_{tun} < 1$ ps, the resonance leading to the peak at eKE = 0.55 eV will be near the lowest RCB saddle point (as previously seen for the fluorescein dianion)[28], which is energetically close to the calculated RCB height of 0.57 eV. The RCB for a plane perpendicular to the nucleobase was also computed (see Figure S3 of the supporting information), but the emission barrier along the *yz* plane was found to be higher than that of the *xz* plane.

While the signal at 0.55 eV is consistent with tunneling through the RCB, it may also arise from direct detachment or autodetachment from the $^1\pi\pi^*$ states. We explored these possibilities by measuring the PE over a range of photon energies from 4.43 to 4.77 eV (280 to 260 nm) as shown in Figure 3(b). The PE peak at eKE = 0.55 eV does not shift despite the change in *hv* by 0.34 eV, which should be readily observable. This observation excludes direct detachment. Autodetachment could still be consistent, but in that case, the electron simply tunnels through a different potential barrier and does not affect the following arguments concerning the angular distributions. Finally, we briefly comment on the possibility that the peak at 0.55 eV arises from thermionic emission (i.e. statistical electron emission from the ground state of the dianion following internal conversion from the $^1\pi\pi^*$ states). After all, some ground state recovery does take place as shown by Cercola *et al.*.[17] We have delayed an electronic gate on the detector to show that all electron emission takes place within 100 ns, thus excluding thermionic emission which proceeds on a much longer timescale. Moreover, the photoelectron spectrum and angular distribution would be inconsistent with such a process.

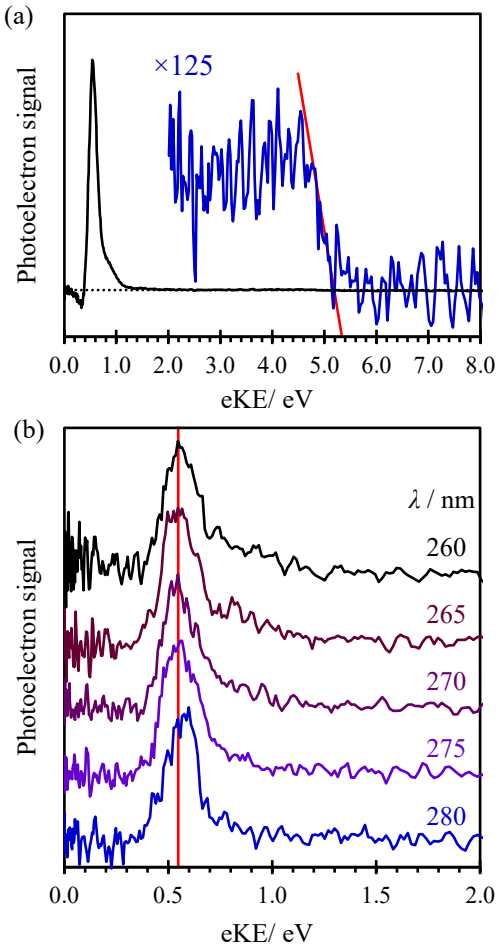

Figure 3: PE spectra of $[ATP–H_2]^{2-}$ taken with (a) focused 4.66 eV femtosecond light and (b) variable wavelength nanosecond light. In (a), a resonance enhanced 2-photon photoelectron spectrum is obtained. the red line shows the high eKE edge of the photoelectron spectrum which intersects the 0 signal (dashed line) at ~5.2 eV. In (b) the red line shows the position of 0.55 eV and highlights that the change in wavelength does not lead to a change in photoelectron spectrum of the tunneling peak.

An electron produced by tunneling will subsequently move along a trajectory determined by the RCB. Given the RCB in Figure 2(a), intuition suggests that such a trajectory will avoid the high potential associated with the phosphate groups. The PE image inset in Figure 1(b), in principle, contains this directional information. The resonance initially excited on the nucleobase involves the optically bright states of adenine, the $^1\pi\pi^*$ states.[44-46] Our calculations show that the transition with the highest oscillator

strength is of this character (details in supporting information). Upon excitation with linearly polarized light of polarization, **ε**, only those $[ATP–H_2]^{2–}$ molecules within a $\cos^2\varphi$ distribution will be excited, where φ is the angle between **ε** and the transition dipole moment (TDM). In Figure 2, $[ATP–H_2]^{2–}$ has been aligned in such a way that the vertical axis (z) is aligned with the TDM of the brightest transition. Hence, from Figure 2, we anticipate that the PE will be emitted predominantly parallel to **ε**. This is consistent with the PE image in Figure 1(b) and its positive β_2 value.

In principle, one could simulate the emission using classical molecular dynamics of an electron under the influence of the RCB.[47] However, we refrain from performing such a simulation here because there are several factors that would undermine such a quantitative prediction and potentially even the qualitative reasoning provided thus far. Firstly, the ions are thermalized at ~300 K and therefore, rotational motion of the $[ATP–H_2]^{2–}$ could blur the alignment.[30] Based on the computed rotational constants, the rotational dephasing time[48] of $[ATP–H_2]^{2–}$ at 300 K is 5 ps and exceeds τ_{tun} by at least one order of magnitude. Hence, rotational motion will not be a significant factor. Secondly, at ~300 K a number of isomers could be present in the gas-phase sample. Infrared multiphoton dissociation experiments and calculations show that $[ATP–H_2]^{2–}$ is predominantly αβ deprotonated, and that it forms an intra-molecular hydrogen bond between the β phosphate and a neighboring oxygen atom.[15, 16, 34] Thirdly, even if a single dominant isomer was present, significant thermal motion could be associated with the phosphates, which could lead to dramatic changes in the RCB. Figure 4 shows the results of a ground state *ab initio* molecular dynamics simulation over 4 ps (details in Section S1.3). This shows the conformational flexibility of $[ATP–H_2]^{2–}$ around the minimum energy structure. Inset is the root mean squared deviation (RMSD) calculated along the simulation time. While the phosphates clearly move, their location relative to the adenine remains quite similar and therefore will not qualitatively affect the RCB and thus also not the angular distribution of the emitted electrons. Fourthly, as demonstrated by the results of Cercola *et al.*[17], excited state dynamics compete with tunneling. On the ground state potential

energy surface, $[ATP–H_2]^{2–}$ dissociates rather than losing an electron,[17] so this cannot contribute to the PE signal. However, substantial nuclear motion clearly takes place on the $^1\pi\pi^*$ states, and $^1n\pi^*$ states may also be involved in the decay mechanism.[46, 49-51] The nuclear dynamics are likely not to have a major impact on the photoelectron angular distribution because the relative position of the phosphates to the nucleobase do not change significantly over the timescale of the dynamics (lifetime is 190 fs). Electronic dynamics on the other hand will alter the relevant molecular orbitals that should be considered. For example, in the case of an $^1n\pi^*$ state, the orbital from which the electron is removed will differ as will the final states in $[ATP–H_2]^–$. The former could be accounted for by calculating the RCB for loss of an electron from the non-bonded orbital located on the amino nitrogen atom. The consequence of this should be reflected in a different final eKE of the emitted electron. Note that Figure 1(b) (and Figure 3(b)) shows a shoulder to higher eKE, which also has a slightly reduced anisotropy ($\beta_2 = +0.48\pm0.33$, where the much larger error reflects the reduced signal intensity). This feature could be consistent with emission from the $^1n\pi^*$ state, although there would also be a different RCB associated with such a process and thus different lifetime, which is not seen in the experiment; we stress that the data is not of sufficient quality at present to be assertive on this conclusion. Alternatively, the shoulder could also arise from hot-bands and/or different isomers, or from direct- and/or autodetachment. It is interesting to notice that in Figure 3(b), the shoulder appears to become more prominent as *hv* increases. This observation is very reminiscent of the behavior in the fluorescein dianion,[28] where direct detachment contributes once the lowest saddle point of the RCB is surpassed.

The above discussion shows that MD simulations would provide only limited added insight. In any case, such simulations would only be feasible if a high level of approximation (e.g. no conformational space investigation, low-dimensional analytical potentials, poor level of theory) would be considered, which in turn lowers the significance of any quantitative results. Despite the complications highlighted above, we can conclude that, following photoexcitation to the $^1\pi\pi^*$ states, resonance-tunneling in [ATP–

$H_2]^{2-}$ is qualitatively consistent with emission from the amino group of adenine. Moreover, it provides a crude structural measure of isolated $[ATP–H_2]^{2-}$ by showing that the negative charges are located on phosphate groups and that these are located around the sugar. This latter observation is in agreement with IR multiphoton dissociation spectra of $[ATP–H_2]^{2-}$ and computational work.[15, 16, 34] Tunneling detachment from the amino groups is expected to result in a β_2 that approaches +2. The reduced value observed here likely arises from the fact that the phosphate lies out of the *xz* plane (Figure 4) which will impose a Coulombic force on the outgoing electron along the *y* axis, thus reducing the overall anisotropy observed experimentally.

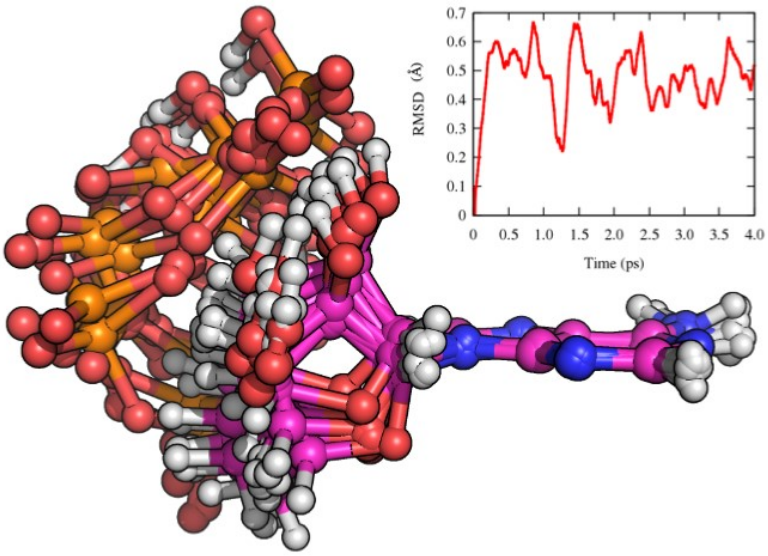

Figure 4: Superimposition of equidistant (every 100 fs) 10 $[ATP–H_2]^{2-}$ geometries along the first ps of the *ab initio* molecular dynamics simulation. Inset is the root mean squared deviation (RMSD) calculated along the 4 ps ground state dynamics.

The above observations of electron tunneling following photoexcitation of adenine in a polyanionic system potentially offer some insight into the photoemission observed in larger DNA complexes studied by the Gabelica and Dugourd groups.[18, 31-33] Specifically, they studied polyanions of

6- and 20-mer single strands and 12-base pair double strands,[31, 32] as well as a 4-tetrad G-quadruplex.[33] A general conclusion of their work is that only the purine nucleobases (adenine and guanine) appear to show enhanced electron emission compared to dissociation: for homo-base 6-mer single strand, this was observed over the $^1\pi\pi^*$ absorption band regardless of charge state (from −2 to −4).[18] The Kappes group have also measured the PE spectra at 4.66 eV for the −3 charge state of the homo-base 6-mer single strands.[37] However, these are difficult to interpret without knowledge of which features arise from direct detachment and which from tunneling. Note that even if a resonance is above the RCB saddle point, it may still be subject to emission by tunneling as shown for the fluorescein dianion[28] and the bisdisulizole tetraanion.[27] Very recently, Daly *et al.* have shown that electron circular dichroism can be observed for chiral DNA strands.[39] Here, we show that tunneling may be efficient in DNA fragments and that PE imaging may offer some insight into the emission process.

Our method provides a new route to understanding photo-oxidation sites and overall structures of polyanions. Looking ahead, reducing the internal temperature of $[ATP–H_2]^{2–}$ using cryogenic ion traps will provide a more controlled environment[52, 53] and may enable quantitative determination of the emission process. A computational perspective on the excited states dynamics of the molecule may in the end allow to obtain a complete picture on the photo-oxidation of this molecule.

Experimental details

The details of the TR-PEI instrument can be found elsewhere.[54, 55] A ∼1 mM methanolic solution of adenosine-5′-triphosphate disodium salt (Sigma Aldrich, UK), was pushed through a syringe and introduced in the first vacuum region through a capillary. A potential gradient led the ions through a series of ring-electrode ion guides, until they reached a pulsed ion trap. Ions were ejected and focused into a collinear Wiley–McLaren time-of-flight mass spectrometer[56] at 10 Hz. At the focus of the mass-

spectrometer, a mass-selected ion packet was irradiated with laser pulses either from a commercial Ti:Sapphire laser (producing femtosecond pulses) or a Nd:YAG pumped OPO (producing nanosecond pulses). For time-resolved measurements, the third harmonic of the fundamental at 1.55 eV was used as a pump pulse and the fundamental as a probe. The time-resolution of the experiment was ~100 fs. Following the interaction of the light with the ion packet, emitted photoelectrons were collected and imaged by a perpendicular VMI arrangement.[57] A 300 ns electronic gate was applied to the microchannel plates so that only signal over this window was collected. PE spectra were obtained from the PE images using polar onion peeling.[58] The PE images were calibrated using the well-known PE image of I^-. The spectral resolution was approximately ~5% of the kinetic energy.

Computational details

$[ATP–H_2]^{2-}$ was optimized with the Møller-Plesset second-order perturbation theory using the resolution of identity approximation (RI-MP2)[59] and the def2-TZVP basis set.[60] The ground state energy was then refined with the def2-QZVP[60] basis set. The first five excitation energies were obtained with the Algebraic Diagrammatic Construction scheme for the polarization propagator at the second order (ADC(2))[61] method and the same def2-QZVP[60] basis set. The RCB was calculated using the Local Static Approximation model,[62] in which the energy for the monoanion plus a point-charge electron (in the geometry of the $[ATP–H_2]^{2-}$) was calculated with an interval of 0.5 Å. Two planes (*xz* and yz) were considered, which pass through the transition dipole moment vector connecting the S_0 and S_2 state. RCB calculations were performed at MP2/def2-SVP level of theory. Ground state *ab initio* molecular dynamics were carried out at B3LYP[63, 64]/aug-cc-pVDZ[65] level of theory, starting from the $[ATP–H_2]^{2-}$ minimum energy geometry. Further computational details are given in Section S.1 of the supporting information.

Supporting Information

Computational details and results of calculations on ground state optimization and excited states; repulsive Coulomb barrier; and ab initio molecular dynamics.

Acknowledgements

This work was supported by funding from the European Union's Horizon 2020 research and innovation program under the Marie Sklodowska-Curie grant agreement No.765266 (LightDyNAmics). D.A. and L.G. thank the University of Vienna and the Vienna Scientific Cluster (VSC) for allocation of computational resources.

References

1. Bruice, P. Y., *Essential organic chemistry*. Third edition. ed.; Pearson: Upper Saddle River, New Jersey, 2016; p xxiv, 644 pages, 26 variously paged.

2. McMurry, J.; Begley, T. P., *The organic chemistry of biological pathways*. Second edition. ed.; Roberts and Company Publishers: Greenwood Village, Colorado, 2016; p pages cm.

3. Stavros, V. G.; Verlet, J. R. R., Gas-Phase Femtosecond Particle Spectroscopy: A Bottom-Up Approach to Nucleotide Dynamics. *Annu. Rev. Phys. Chem.* **2016,** *67* (1), 211-232.

4. Weber, J. M.; Marcum, J.; Nielsen, S. B., UV Photophysics of DNA and RNA Nucleotides In Vacuo: Dissociation Channels, Time Scales, and Electronic Spectra. In *Photophysics of Ionic Biochromophores*, Brøndsted Nielsen, S.; Wyer, J. A., Eds. Springer Berlin Heidelberg: Berlin, Heidelberg, 2013; pp 181-207.

5. Satzger, H.; Townsend, D.; Zgierski, M. Z.; Patchkovskii, S.; Ullrich, S.; Stolow, A., Primary processes underlying the photostability of isolated DNA bases: Adenine. *Proc. Natl. Acad. Sci. U.S.A.* **2006,** *103* (27), 10196-10201.

6. Bisgaard, C. Z.; Satzger, H.; Ullrich, S.; Stolow, A., Excited-State Dynamics of Isolated DNA Bases: A Case Study of Adenine. *ChemPhysChem* **2009,** *10* (1), 101-110.

7. Wells, K. L.; Hadden, D. J.; Nix, M. G. D.; Stavros, V. G., Competing πσ* States in the Photodissociation of Adenine. *J. Phys. Chem. Lett.* **2010,** *1* (6), 993-996.

8. Mai, S.; Richter, M.; Marquetand, P.; González, L., Excitation of Nucleobases from a Computational Perspective II: Dynamics. In *Photoinduced Phenomena in Nucleic Acids I: Nucleobases in the Gas Phase and in Solvents*, Barbatti, M.; Borin, A. C.; Ullrich, S., Eds. Springer International Publishing: Cham, 2015; pp 99-153.

9. Chatterley, A. S.; West, C. W.; Stavros, V. G.; Verlet, J. R. R., Time-resolved photoelectron imaging of the isolated deprotonated nucleotides. *Chem. Sci.* **2014,** *5* (10), 3963-3975.

10. Chatterley, A. S.; West, C. W.; Roberts, G. M.; Stavros, V. G.; Verlet, J. R. R., Mapping the Ultrafast Dynamics of Adenine onto Its Nucleotide and Oligonucleotides by Time-Resolved Photoelectron Imaging. *J. Phys. Chem. Lett.* **2014,** *5* (5), 843-848.

11. Yang, X.; Wang, X.-B.; Vorpagel, E. R.; Wang, L.-S., Direct experimental observation of the low ionization potentials of guanine in free oligonucleotides by using photoelectron spectroscopy. *Proc. Natl. Acad. Sci. U.S.A.* **2004,** *101* (51), 17588-17592.

12. Parker, A. W.; Quinn, S. J., Infrared Spectroscopy of DNA. In *Encyclopedia of Biophysics*, Roberts, G. C. K., Ed. Springer Berlin Heidelberg: Berlin, Heidelberg, 2013; pp 1065-1074.

13. Keane, P. M.; Baptista, F. R.; Gurung, S. P.; Devereux, S. J.; Sazanovich, I. V.; Towrie, M.; Brazier, J. A.; Cardin, C. J.; Kelly, J. M.; Quinn, S. J., Long-Lived Excited-State Dynamics of i-Motif Structures Probed by Time-Resolved Infrared Spectroscopy. *ChemPhysChem* **2016,** *17* (9), 1281-1287.

14. Hall, J. P.; Poynton, F. E.; Keane, P. M.; Gurung, S. P.; Brazier, J. A.; Cardin, D. J.; Winter, G.; Gunnlaugsson, T.; Sazanovich, I. V.; Towrie, M.; Cardin, C. J.; Kelly, J. M.; Quinn, S. J., Monitoring one-electron photo-oxidation of guanine in DNA crystals using ultrafast infrared spectroscopy. *Nature Chem.* **2015,** *7* (12), 961-967.

15. Ligare, M. R.; Rijs, A. M.; Berden, G.; Kabeláč, M.; Nachtigallova, D.; Oomens, J.; de Vries, M. S., Resonant Infrared Multiple Photon Dissociation Spectroscopy of Anionic Nucleotide Monophosphate Clusters. *J. Phys. Chem. B* **2015,** *119* (25), 7894-7901.

16. van Outersterp, R. E.; Martens, J.; Berden, G.; Steill, J. D.; Oomens, J.; Rijs, A. M., Structural characterization of nucleotide 5′ -triphosphates by infrared ion spectroscopy and theoretical studies. *Phys. Chem. Chem. Phys.* **2018,** *20* (44), 28319-28330.

17. Cercola, R.; Matthews, E.; Dessent, C. E. H., Photoexcitation of Adenosine 5′ -Triphosphate Anions in Vacuo: Probing the Influence of Charge State on the UV Photophysics of Adenine. *J. Phys. Chem. B* **2017,** *121* (22), 5553-5561.

18. Daly, S.; Porrini, M.; Rosu, F.; Gabelica, V., Electronic spectroscopy of isolated DNA polyanions. *Faraday Discuss.* **2019,** *217* (0), 361-382.

19. Wang, X.-B.; Ding, C.-F.; Wang, L.-S., Photodetachment Spectroscopy of a Doubly Charged Anion: Direct Observation of the Repulsive Coulomb Barrier. *Phys. Rev. Lett.* **1998,** *81*, 3351-3354.

20. Simons, J., Molecular Anions. *J. Phys. Chem. A* **2008,** *112* (29), 6401-6511.

21. Dreuw, A.; Cederbaum, L. S., Multiply Charged Anions in the Gas Phase. *Chem. Rev.* **2002,** *102* (1), 181-200.

22. Verlet, J. R. R.; Horke, D. A.; Chatterley, A. S., Excited states of multiply-charged anions probed by photoelectron imaging: riding the repulsive Coulomb barrier. *Phys. Chem. Chem. Phys.* **2014,** *16* (29), 15043-15052.

23. Scheller, M. K.; Compton, R. N.; Cederbaum, L. S., Gas-Phase Multiply Charged Anions. *Science* **1995,** *270* (5239), 1160-1166.

24. Wang, L.-S.; Wang, X.-B., Probing Free Multiply Charged Anions Using Photodetachment Photoelectron Spectroscopy. *J. Phys. Chem. A* **2000,** *104* (10), 1978-1990.

25. Wang, X.-B.; Wang, L.-S., Observation of negative electron-binding energy in a molecule. *Nature* **1999,** *400* (6741), 245-248.

26. Wang, X.-B.; Woo, H.-K.; Huang, X.; Kappes, M. M.; Wang, L.-S., Direct Experimental Probe of the On-Site Coulomb Repulsion in the Doubly Charged Fullerene Anion $\mathrm{C}_{70}{}^{2\ensuremath{-}}$. *Phys. Rev. Lett.* **2006,** *96* (14), 143002.

27. Dau, P. D.; Liu, H.-T.; Yang, J.-P.; Winghart, M.-O.; Wolf, T. J. A.; Unterreiner, A.-N.; Weis, P.; Miao, Y.-R.; Ning, C.-G.; Kappes, M. M.; Wang, L.-S., Resonant tunneling through the repulsive Coulomb barrier of a quadruply charged molecular anion. *Phys. Rev. A* **2012,** *85* (6), 064503.

28. Horke, D. A.; Chatterley, A. S.; Verlet, J. R., Effect of internal energy on the repulsive Coulomb barrier of polyanions. *Phys. Rev. Lett.* **2012,** *108* (8), 083003.

29. Xing, X.-P.; Wang, X.-B.; Wang, L.-S., Photoelectron imaging of multiply charged anions: Effects of intramolecular Coulomb repulsion and photoelectron kinetic energies on photoelectron angular distributions. *J. Chem. Phys.* **2009,** *130* (7), 074301.

30. Horke, D. A.; Chatterley, A. S.; Verlet, J. R. R., Femtosecond Photoelectron Imaging of Aligned Polyanions: Probing Molecular Dynamics through the Electron–Anion Coulomb Repulsion. *J. Phys. Chem. Lett.* **2012,** *3* (7), 834-838.

31. Gabelica, V.; Tabarin, T.; Antoine, R.; Rosu, F.; Compagnon, I.; Broyer, M.; De Pauw, E.; Dugourd, P., Electron photodetachment dissociation of DNA polyanions in a quadrupole ion trap mass spectrometer. *Anal. Chem.* **2006,** *78* (18), 6564-72.

32. Gabelica, V.; Rosu, F.; Tabarin, T.; Kinet, C.; Antoine, R.; Broyer, M.; De Pauw, E.; Dugourd, P., Base-dependent electron photodetachment from negatively charged DNA strands upon 260-nm laser irradiation. *J. Am. Chem. Soc.* **2007,** *129* (15), 4706-13.

33. Rosu, F.; Gabelica, V.; De Pauw, E.; Antoine, R.; Broyer, M.; Dugourd, P., UV spectroscopy of DNA duplex and quadruplex structures in the gas phase. *J. Phys. Chem. A* **2012,** *116* (22), 5383-91.

34. Schinle, F.; Crider, P. E.; Vonderach, M.; Weis, P.; Hampe, O.; Kappes, M. M., Spectroscopic and theoretical investigations of adenosine 5'-diphosphate and adenosine 5'-triphosphate dianions in the gas phase. *Phys. Chem. Chem. Phys.* **2013,** *15* (18), 6640-50.

35. Burke, R. M.; Dessent, C. E. H., Effect of Cation Complexation on the Structure of a Conformationally Flexible Multiply Charged Anion: Stabilization of Excess Charge in the Na+·Adenosine 5′ -Triphosphate Dianion Ion-Pair Complex. *J. Phys. Chem. A* **2009,** *113* (12), 2683-2692.

36. Burke, R. M.; Pearce, J. K.; Boxford, W. E.; Bruckmann, A.; Dessent, C. E. H., Stabilization of Excess Charge in Isolated Adenosine 5‘-Triphosphate and Adenosine 5‘-Diphosphate Multiply and Singly Charged Anions. *J. Phys. Chem. A* **2005,** *109* (43), 9775-9785.

37. Vonderach, M.; Ehrler, O. T.; Matheis, K.; Weis, P.; Kappes, M. M., Isomer-Selected Photoelectron Spectroscopy of Isolated DNA Oligonucleotides: Phosphate and Nucleobase Deprotonation at High Negative Charge States. *J. Am. Chem. Soc.* **2012,** *134* (18), 7830-7841.

38. Weber, J. M.; Ioffe, I. N.; Berndt, K. M.; Löffler, D.; Friedrich, J.; Ehrler, O. T.; Danell, A. S.; Parks, J. H.; Kappes, M. M., Photoelectron Spectroscopy of Isolated Multiply Negatively Charged Oligonucleotides. *J. Am. Chem. Soc.* **2004,** *126* (27), 8585-8589.

39. Daly, S.; Rosu, F.; Gabelica, V., Mass-resolved electronic circular dichroism ion spectroscopy. *Science* **2020,** *368* (6498), 1465-1468.

40. Reid, K. L., Photoelectron angular distributions. *Annu. Rev. Phys. Chem.* **2003,** *54*, 397-424.

41. Cooper, J.; Zare, R. N., Angular Distribution of Photoelectrons. *J. Chem. Phys.* **1968,** *48* (2), 942-943.

42. Cooper, J.; Zare, R. N., Erratum: Angular Distribution of Photoelectrons. *J. Chem. Phys.* **1968,** *49* (9), 4252-4252.

43. Chatterley, A. S.; Johns, A. S.; Stavros, V. G.; Verlet, J. R. R., Base-Specific Ionization of Deprotonated Nucleotides by Resonance Enhanced Two-Photon Detachment. *J. Phys. Chem. A* **2013,** *117* (25), 5299-5305.

44. Santoro, F.; Improta, R.; Fahleson, T.; Kauczor, J.; Norman, P.; Coriani, S., Relative Stability of the La and Lb Excited States in Adenine and Guanine: Direct Evidence from TD-DFT Calculations of MCD Spectra. *J. Phys. Chem. Lett.* **2014,** *5* (11), 1806-1811.

45. Serrano-Andrés, L.; Merchán, M.; Borin, A. C., A Three-State Model for the Photophysics of Adenine. *Chem. Eur. J.* **2006,** *12* (25), 6559-6571.

46. Conti, I.; Garavelli, M.; Orlandi, G., Deciphering Low Energy Deactivation Channels in Adenine. *J. Am. Chem. Soc.* **2009,** *131* (44), 16108-16118.

47. West, C. W.; Bull, J. N.; Woods, D. A.; Verlet, J. R. R., Photoelectron imaging as a probe of the repulsive Coulomb barrier in the photodetachment of antimony tartrate dianions. *Chem. Phys. Lett.* **2016,** *645*, 138-143.

48. Blokhin, A. P.; Gelin, M. F.; Khoroshilov, E. V.; Kryukov, I. V.; Sharkov, A. V., Dynamics of optically induced anisotropy in an ensemble of asymmetric top molecules in the gas phase. *Opt. Spectrosc.* **2003,** *95* (3), 346-352.

49. Conti, I.; Nenov, A.; Höfinger, S.; Flavio Altavilla, S.; Rivalta, I.; Dumont, E.; Orlandi, G.; Garavelli, M., Excited state evolution of DNA stacked adenines resolved at the CASPT2//CASSCF/Amber level: from the bright to the excimer state and back. *Phys. Chem. Chem. Phys.* **2015,** *17* (11), 7291-7302.

50. Conti, I.; Di Donato, E.; Negri, F.; Orlandi, G., Revealing Excited State Interactions by Quantum-Chemical Modeling of Vibronic Activities: The R2PI Spectrum of Adenine. *J. Phys. Chem. A* **2009,** *113* (52), 15265-15275.

51. Picconi, D.; Avila Ferrer, F. J.; Improta, R.; Lami, A.; Santoro, F., Quantum-classical effective-modes dynamics of the ππ* → nπ* decay in 9H-adenine. A quadratic vibronic coupling model. *Faraday Discuss.* **2013,** *163* (0), 223-242.

52. Wang, X. B.; Wang, L. S., Development of a low-temperature photoelectron spectroscopy instrument using an electrospray ion source and a cryogenically controlled ion trap. *Rev. Sci. Instrum.* **2008,** *79* (7), 073108.

53. Garand, E., Spectroscopy of Reactive Complexes and Solvated Clusters: A Bottom-Up Approach Using Cryogenic Ion Traps. *J. Phys. Chem. A* **2018,** *122* (32), 6479-6490.

54. Lecointre, J.; Roberts, G. M.; Horke, D. A.; Verlet, J. R. R., Ultrafast Relaxation Dynamics Observed Through Time-Resolved Photoelectron Angular Distributions. *J. Phys. Chem. A* **2010,** *114* (42), 11216-11224.

55. Stanley, L. H.; Anstöter, C. S.; Verlet, J. R. R., Resonances of the anthracenyl anion probed by frequency-resolved photoelectron imaging of collision-induced dissociated anthracene carboxylic acid. *Chem. Sci.* **2017,** *8* (4), 3054-3061.

56. Wiley, W. C.; McLaren, I. H., Time‐of‐Flight Mass Spectrometer with Improved Resolution. *Rev. Sci. Instrum.* **1955,** *26* (12), 1150-1157.

57. Horke, D. A.; Roberts, G. M.; Lecointre, J.; Verlet, J. R. R., Velocity-map imaging at low extraction fields. *Rev. Sci. Instrum.* **2012,** *83* (6), 063101.

58. Roberts, G. M.; Nixon, J. L.; Lecointre, J.; Wrede, E.; Verlet, J. R. R., Toward real-time charged-particle image reconstruction using polar onion-peeling. *Rev. Sci. Instrum.* **2009,** *80* (5), 053104.

59. Weigend, F.; Häser, M., RI-MP2: first derivatives and global consistency. *Theor. Chem. Acc.* **1997,** *97* (1), 331-340.

60. Weigend, F., Accurate Coulomb-fitting basis sets for H to Rn. *Phys. Chem. Chem. Phys.* **2006,** *8* (9), 1057-1065.

61. Dreuw, A.; Wormit, M., The algebraic diagrammatic construction scheme for the polarization propagator for the calculation of excited states. *Wiley Interdiscip. Rev. Comput. Mol. Sci.* **2015,** *5* (1), 82-95.

62. Dreuw, A.; Cederbaum, L. S., Erratum: Nature of the repulsive Coulomb barrier in multiply charged negative ions [Phys. Rev. A 63, 012501 (2000)]. *Phys. Rev. A* **2001,** *63* (4), 049904.

63. Becke, A. D., Density‐functional thermochemistry. III. The role of exact exchange. *J. Chem. Phys.* **1993,** *98* (7), 5648-5652.

64. Lee, C.; Yang, W.; Parr, R. G., Development of the Colle-Salvetti correlation-energy formula into a functional of the electron density. *Phys. Rev. B* **1988,** *37* (2), 785-789.

65. Kendall, R. A.; Jr., T. H. D.; Harrison, R. J., Electron affinities of the first‐row atoms revisited. Systematic basis sets and wave functions. *J. Chem. Phys.* **1992,** *96* (9), 6796-6806.